Theoretical Studies on the Structures, Thermodynamic Properties, Detonation Properties, and Pyrolysis Mechanisms of Spiro Nitramines

Ling Qiu, Heming Xiao,* Xuedong Gong, Xuehai Ju, and Weihua Zhu

Department of Chemistry, Nanjing University of Science and Technology, Nanjing 210094, People's Republic of China

Received: July 28, 2005; In Final Form: December 26, 2005

Density function theory (DFT) has been employed to study the geometric and electronic structures of a series of spiro nitramines at the B3LYP/6-31G** level. The calculated results agree reasonably with available experimental data. Thermodynamic properties derived from the infrared spectra on the basis of statistical thermodynamic principles are linearly correlated with the number of nitramine groups as well as the temperature. Detonation performances were evaluated by the Kamlet-Jacobs equations based on the calculated densities and heats of formation. It is found that some compounds with the predicted densities of ca. 1.9 g/cm^3, detonation velocities over 9 km/s, and detonation pressures of about 39 GPa (some even over 40 GPa) may be novel potential candidates of high energy density materials (HEDMs). Thermal stability and the pyrolysis mechanism of the title compounds were investigated by calculating the bond dissociation energies (BDE) at the B3LYP/6-31G** level and the activation energies (E_a) with the selected PM3 semiempirical molecular orbital (MO) based on the unrestricted Hartree−Fock model. The relationships between BDE, E_a, and the electronic structures of the spiro nitramines were discussed in detail. Thermal stabilities and decomposition mechanisms of the title compounds derived from the B3LYP/6-31G** BDE and the UHF−PM3 E_a are basically consistent. Considering the thermal stability, TNSHe (tetranitrotetraazaspirohexane), TNSH (tetranitrotetraazaspiroheptane), and TNSO (tetranitrotetraazaspirooctane) are recommended as the preferred candidates of HEDMs. These results may provide basic information for the molecular design of HEDMs.

1. Introduction

Nowadays, high energy density materials (HEDMs) have been receiving considerable attention because of their superior explosive performances over the currently used materials. Searching for novel HEDMs to meet the future demands has become one of the most activated regions and seems to be never-ending. As is well-known, nitramines have had important applications in both civilian and military fields for a long time. This group of compounds is still a source of explosives or propellants that possess predominantly high energy contents.[1−3] At present, the attractive nitramine involves a series of (poly)-cyclic nitramines. The ongoing research work on the syntheses of such compounds is based on the fact that they are denser than their open-structured counterparts and their higher densities result in higher detonation velocities and pressures, because the detonation velocity and pressure increase proportionally with the density and square of it, respectively.[4] The reported syntheses of TNAD (tetranitrotetraazadecalin)[5] and HNIW (hexanitrohexaazaisowurtzitane)[6] are the results of efforts in this direction to develop energetic materials with improved crystalline densities and high stored energies to meet superior performance requirements. They appear to be the future candidates to compete with the currently used HEDMs such as HMX (1,3,5,7-tetranitro-1,3,5,7-tetraazacyclooctane).

Recently, another type of polycyclic nitramine, spirobicyclic nitramines such as TNSD (tetranitrotetraazaspirodecane)[7] and TNSU (tetranitrotetraazaspiroundecane),[8−10] which are formed by two nitroaza rings sharing a common carbon atom, were investigated as promising candidates of HEDMs. To date, there have been a series of experimental studies on TNSD and TNSU. For example, Willer determined the density of TNSD to be 1.70 g/cm^3.[5] Lowe-Ma also measured the densities and impact sensitivities of TNSD and TNSU[11] and compared them with the representative nitramine explosives such as RDX and HMX. He found that TNSD and TNSU (impact sensitivities of 50 and 60 cm, respectively) are much less sensitive to impact than RDX and HMX (25−28 and 18−26 cm, respectively), but their densities are not large (1.71 and 1.74 g/cm^3 for TNSD and TNSU, respectively). Their crystal structures and thermal decomposition have been studied by Lowe-Ma et al.[11,12] and Brill et al.,[13,14] respectively. However, to the best of our knowledge, there are few theoretical studies on them except one of our recent studies,[15] and no investigations on the other spiro nitramines have been reported until now. This may be attributed to the low densities of TNSD and TNSU, which exclude them from further investigation. As is well-known, with the rapid development on the computer technology and theoretical chemistry, identification of the compounds that have significant advantages over the currently used materials could be facilitated and more economical with computer modeling and simulating. Quantitative estimation of properties, such as the heat of formation, density, detonation velocity, detonation pressure, and sensitivity, would permit the selection of the most promising substances for laboratory synthesis and further consideration. We have a continuing program to attempt to understand the interrelationships between the structures and detonation performances of the energetic cyclic nitramines and to provide useful information for the molecular design of new

* Corresponding author. Fax: +86−25−84303919. E-mail: xiao@mail.njust.edu.cn.

10.1021/jp054169g CCC: $33.50
Published on Web 02/14/2006

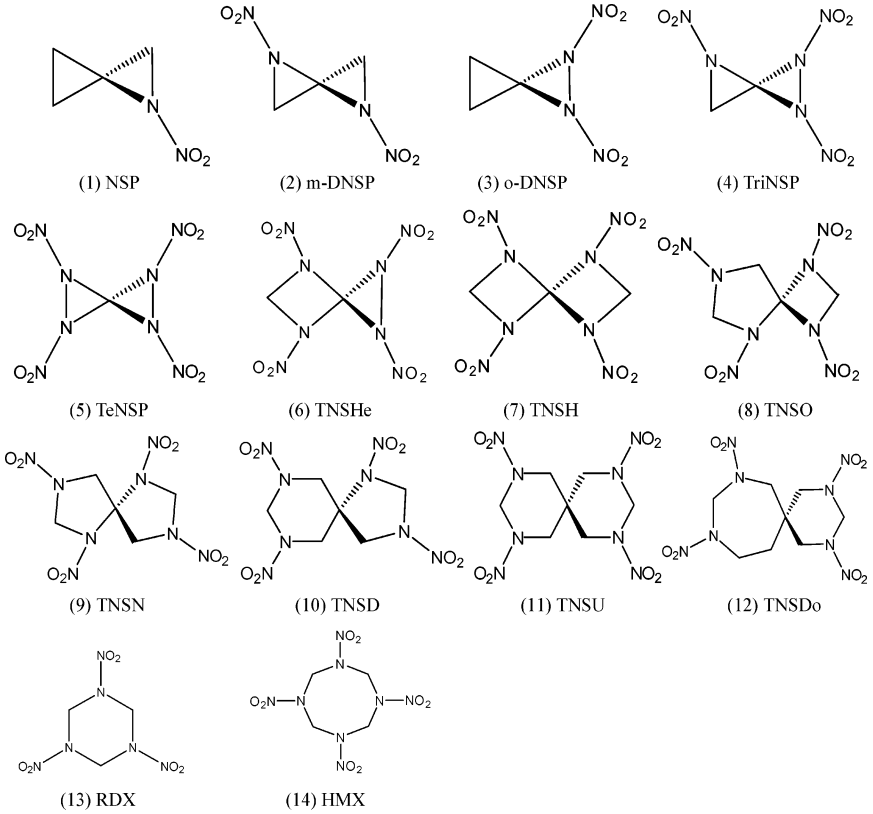

Figure 1. Illustration of the molecular structures of the spiro nitramines (**1**−**12**) studied in this research, RDX, and HMX (hydrogen atoms are omitted for clarity).

energetic materials.[15−19] Here, motivated by and based on the previous studies on TNSD and TNSU, we performed density functional theory (DFT)[20] investigations on a series of spiro bicyclic nitramines designed on the basis of the experimentally determined structures of TNSD and TNSU (see Figure 1 for the structural diagrams of these spiro nitramines). We look forward to finding out novel potential candidates of HEDMs in this group of compounds. According to the nomenclature of TNSD and TNSU, the following similar abbreviations were used for brevity: (1) 1-nitroazaspiropentane (NSP), (2) 1,3-dinitrodiazaspiropentane (*m*-DNSP), (3) 1,2-dinitrodiazaspiropentane (*o*-DNSP), (4) trinitrotriazaspiropentane (TriNSP), (5) tetranitrotetraazaspiropentane (TeNSP), (6) tetranitrotetraazaspirohexane (TNSHe), (7) tetranitrotetraazaspiroheptane (TNSH), (8) tetranitrotetraazaspirooctane (TNSO), (9) tetranitrotetraazaspirononane (TNSN), (10) tetranitrotetraazaspirodecane (TNSD), (11) tetranitrotetraazaspiroundecane (TNSU), and (12) tetranitrotetraazaspirododecane (TNSDo). Meanwhile, we also performed theoretical calculations on RDX and HMX at the same level to provide benchmarks on the detonation performances and thermal stability.

In this paper, geometric features, electronic structures, thermodynamic properties, and detonation performances have been systematically studied for twelve spiro nitramines using theoretical approaches. Results of different structures were compared, and the relationships between the structures and various properties were analyzed. In addition, thermal stabilities and pyrolysis mechanisms were evaluated from the bond dissociation energies (BDE) and the activation energies (E_a) of the initial step in the pyrolysis reactions according to the previous studies.[3,18,19,21−28] The calculated results show that some of our studied spiro nitramines can be used as HEDMs.

Another set of useful data obtained from the DFT calculations are the fundamental vibrational frequencies. These were calculated for the title compounds using analytical second-order derivatives at the optimized geometries. The theoretical frequencies should be compared to the gas-phase experimental results measured under low pressure; however, hitherto we are not aware of any experimental measurements of the vibrational frequencies reported. So, we hope that the computed vibrational frequencies will stimulate experimental investigations of the gas-phase vibrational spectroscopies of the interesting molecules and can be used as references in their detection in the reaction mixtures for the experimentalists.

The organization of this paper is as follows. First, the computational methodology is described in section 2. Results and discussion are presented in section 3, including geometric structures (subsection 3.1), bond overlap population analysis (subsection 3.2), thermodynamic properties (subsection 3.3), detonation parameters (subsection 3.4), and thermal stability and pyrolysis mechanism (subsection 3.5). Finally, the main conclusions are summarized in section 4.

2. Computational Methods

All the molecules in Figure 1 and the related radical species generated from the ChemBats3D software were fully optimized without any symmetry restrictions by the Berny method at the DFT-(U)B3LYP level with the 6-31G** basis set.[29−31] To characterize the nature of the stationary points and to determine the zero-point vibrational energy corrections, harmonic vibrational analyses were performed subsequently on each optimized structure at the same level with the *Gaussian 98* program.[32] According to the previous studies, the computed harmonic vibrational frequencies were scaled uniformly by a factor 0.96 to take into account the systematic overestimation of vibrational frequencies in the B3LYP/6-31G** calculations.[33] On the basis of the principle of statistical thermodynamics,[34] heat capacity,

TABLE 1: Methods for Calculating the *N*, $\bar{M}$, and *Q* Parameters of the CaHbOcNd Explosive[a,b]

parameter	stoichiometric ratio		
	$c \geq 2a + b/2$	$2a + b/2 > c \geq b/2$	$b/2 > c$
N	$(b + 2c + 2d)/4M$	$(b + 2c + 2d)/4M$	$(b + d)/2M$
$\bar{M}$	$4M/(b + 2c + 2d)$	$(56d + 88c - 8b)/(b + 2c + 2d)$	$(2b + 28d + 32c)/(b + d)$
Q	$(28.9b + 94.05a + 0.239\Delta H_f^\circ)/M$	$[28.9b + 94.05(c/2 - b/4) + 0.239\Delta H_f^\circ]/M$	$(57.8c + 0.239\Delta H_f^\circ)/M$

[a] CaHbOcNd denotes the compound composed of the C, H, O, and N elements; *a*, *b*, *c*, and *d* stand for the number of C, H, O, and N atoms in the compound. [b] *N* is moles of gaseous detonation products per gram of explosive (in mol/g); $\bar{M}$ is the average molecular weight of the gaseous products (in g/mol); *Q* is the chemical energy of detonation (in kJ/g); *M* in the formula is the molecular weight of the title compounds (in g/mol); ΔH_f° is the standard heat of formation of the studied compound (in kJ/mol).

entropy, and enthalpy ranging from 200 to 800 K were derived from the scaled frequencies.

Density (ρ), detonation velocity (D), and detonation pressure (P) are the important parameters to evaluate the explosive performances of energetic materials and can be predicted by the empirical Kamlet−Jacobs equations[4] as follows:

$$D = 1.01(N\bar{M}^{1/2}Q^{1/2})^{1/2}(1 + 1.30\,\rho) \quad (1)$$

$$P = 1.558\rho^2 N\bar{M}^{1/2}Q^{1/2} \quad (2)$$

where each term in eqs 1 and 2 is defined as follows: D, detonation velocity (km/s); P, detonation pressure (GPa); ρ, density of a compound (g/cm^3); N, moles of gaseous detonation products per gram of explosive; $\bar{M}$, average molecular weight of gaseous products; Q, chemical energy of detonation (kJ/g). Here, the parameters N, $\bar{M}$, and Q were calculated according to the chemical composition of each explosive as listed in Table 1.[4,35] The density of each compound was predicted from the molecular volume divided by molecular weight, while the molecular volume of each molecule was yielded from the statistical average of 100 single-point molar volume calculations for each optimized structure. The molar volume was defined as inside a contour of 0.001 electrons/Bohr^3 density that was evaluated using a Monte Carlo integration implemented in the *Gaussian 98* program. This method has been successfully tested on various CHNO molecules[36] and accurately predicts the densities, detonation velocities, and detonation pressures of the explosives.[15−19,36−39]

To measure the bond strength and relative stabilities of the title compounds, we calculated the BDE of various bond dissociations. BDE is originally defined as the enthalpy change at 298 K and 1 atm for the chemical bond dissociation in a molecule as follows:[40]

$$\mathrm{A{-}B(g)} \rightarrow \mathrm{A^\bullet(g) + B^\bullet(g)} \quad (3)$$

$$\mathrm{BDE(A{-}B)} = \Delta H^\circ = [\Delta H_f^\circ(\mathrm{A^\bullet}) + \Delta H_f^\circ(\mathrm{B^\bullet})] - \Delta H_f^\circ(\mathrm{A{-}B}) \quad (4)$$

where A−B stands for the neutral molecules, A$^\bullet$ and B$^\bullet$ stand for the corresponding product radicals after the bond dissociation, BDE(A−B) is the bond dissociation enthalpy of bond A−B, ΔH° is the standard heat of reaction in the bond dissociation process, $\Delta H_f^\circ(\mathrm{A^\bullet})$, $\Delta H_f^\circ(\mathrm{B^\bullet})$, and $\Delta H_f^\circ(\mathrm{A - B})$ are the standard heats of formation for the products and reactant at 298 K, respectively. However, in the present paper, the BDE is defined as the difference between the zero-point energy corrected total energies at 0 K of the parent nitramines and those of their corresponding radicals in the unimolecular bond dissociations. This has been successfully and frequently used to measure and determine the bond strength and relative stability of the compounds and corresponding radicals.[21−28] Therefore, we computed the BDE at 0 K according to the energy changes of the bond dissociation process at the B3LYP/6-31G** level: $\mathrm{BDE(A{-}B)} = \Delta E = [E(\mathrm{A^\bullet}) + E(\mathrm{B^\bullet})] - E(\mathrm{A{-}B})$. The thermal decomposition mechanism can also be determined from the calculated BDE.

Furthermore, the pyrolysis mechanisms of the spiro nitramines were investigated with a selected semiempirical MO method. As is well-known, it is very difficult to perform calculations on the pyrolysis mechanisms for large systems such as the polycyclic nitramines at high theoretical levels. However, the semiempirical MO methods[41−44] such as PM3, AM1, MNDO, and MINDO/3 with the unrestricted Hartree−Fock (UHF) model can give satisfactory results, and PM3 calculations are rapid and comparatively reliable for organic compounds.[45] So, the UHF−PM3 method incorporated in the MOPAC 6.0 program[46] was applied to investigate the pyrolysis of the title compounds, RDX and HMX. Each transition-state (TS) structure was located and confirmed by both the presence of only one imaginary frequency and the calculation of the intrinsic reaction coordinate (IRC).

All the calculations considered here were performed on a Pentium IV personal computer using the default convergence criteria given in the programs.

3. Results and Discussion

3.1. Geometric Structures. Before discussing the electronic structures, various properties, and bond dissociation energies associated with the spiro nitramines, it is useful to examine the geometric structures for the species concerned. All of the optimized structures are characterized by the harmonic vibrational analyses to be true local energy minima on the potential energy surfaces without any imaginary frequency. The optimized structures of the spiro nitramines and the corresponding bond dissociation products were presented in the Figure 1S of the Supporting Information. For clarity, only the overall ranges of the optimized bond lengths and the molecular symmetries of the title compounds at the B3LYP/6-31G** level were presented in Table 2. The bond angles and dihedral angles can be measured reliably from the X-ray diffraction, and comparable results could be achieved from theoretical calculations. For better comparison and testing of the reliability of the calculated results, available experimental geometric parameters[11,12] of TNSD and TNSU were also listed in Table 2.

On the whole, the optimized structures are in concordance with the experimental observations. Comparisons between the experimental and theoretical bond lengths show that the calculated results are slightly larger than the experimental structures. For example, the observed crystal structures TNSD and TNSU have shorter N−NO$_2$ bonds by ca. 0.02−0.1 Å than the theoretical structures, and the experimental N−O bonds are shorter than the calculated results by about 0.01 Å. The trivial discrepancies are mainly due to the solid-state effect, i.e., intermolecular interactions. Such interactions are not presented in the DFT calculations applied here. Intermolecular electrostatic

TABLE 2: Ranges of the Bond Lengths (Å) for the Title Compounds Optimized at the B3LYP/6-31G Level and Compared with Available Experimental Data[a]**

no.	compds	sym.	C−C	C−N	N−N	N−NO_2	N−O	C−H
1	NSP	C_1	1.475−1.534	1.450, 1.482		1.437	1.222, 1.223	1.085−1.087
2	*m*-DNSP	C_1	1.471, 1.472	1.433−1.488		1.448, 1.455	1.216−1.220	1.086, 1.087
3	*o*-DNSP	D_2	1.472, 1.541	1.435	1.457	1.494	1.207, 1.216	1.085, 1.086
4	TriNSP	C_1	1.467	1.420−1.492	1.458	1.469−1.523	1.203−1.215	1.086, 1.807
5	TeNSP	S_4		1.414	1.461	1.541	1.201, 1.206	
6	TNSHe	C_2		1.432−1.481	1.441	1.422, 1.528	1.201−1.220	1.090
7	TNSH	T_d		1.462, 1.475		1.407	1.220	1.091
8	TNSO	C_1	1.547	1.457−1.484		1.387−1.437	1.219−1.228	1.087−1.092
9	TNSN	C_1	1.555, 1.564	1.454−1.479		1.374−1.437	1.220−1.234	1.086−1.094
10	TNSD	C_1	1.545−1.565	1.452−1.498		1.383−1.481	1.213−1.230	1.084−1.097
			(1.526−1.557)	(1.432−1.469)		(1.347−1.385)	(1.209−1.229)	(0.960)
11	TNSU	C_1	1.541−1.553	1.455−1.463		1.402−1.408	1.223−1.229	1.084−1.104
			(1.514−1.557)	(1.438−1.478)		(1.377−1.388)	(1.211−1.230)	(1.140)
12	TNSDo	C_1	1.539−1.556	1.442−1.476		1.389−1.410	1.223−1.232	1.084−1.102

[a] Values in the parentheses are experimental data.[11,12]

TABLE 3: Ranges of the Bond Overlap Populations for the Title Compounds at the B3LYP/6-31G Level**

no.	compd	C−C	C−N	N−N	N−NO_2	N−O	C−H
1	NSP	0.2274−0.3178	0.1392, 0.1614		0.1854	0.3016, 0.3066	0.3732−0.3863
2	*m*-DNSP	0.2474, 0.2748	0.1182−0.1680		0.1692, 0.1789	0.3010−0.3138	0.3684−0.3844
3	*o*-DNSP	0.1965, 0.3151	0.0955	0.0035	0.1211	0.2930, 0.3201	0.3821, 0.3857
4	TriNSP	0.2831	0.0407−0.1524	−0.0180	0.1119−0.1644	0.2920−0.3229	0.3696, 0.3789
5	TeNSP		0.0885	−0.0409	0.1062	0.2978, 0.3215	
6	TNSHe		0.0639−0.2144	−0.0346	0.0976, 0.1488	0.2960−0.3270	0.3835
7	TNSH		0.1807−0.2128		0.1499−0.1501	0.3147−0.3350	0.3838
8	TNSO	0.3167	0.1686−0.2433		0.1523−0.1682	0.2964−0.3404	0.3667−0.3918
9	TNSN	0.3176, 0.3193	0.1941−0.2408		0.1637−0.1839	0.3123−0.3336	0.3714−0.3903
10	TNSD	0.2943−0.3234	0.1787−0.2535		0.1734−0.1808	0.2927−0.3326	0.3696−0.3980
11	TNSU	0.3113−0.3385	0.2224−0.2518		0.1730−0.1843	0.3116−0.3360	0.3701−0.3979
12	TNSDo	0.3273−0.3574	0.2069−0.2577		0.1737−0.1899	0.3087−0.3368	0.3653−0.3897

interactions[47] contribute to the shorter N−N bonds in the crystal, as mentioned in previous studies for dimethylnitramine[48] and RDX.[24] Donation of lone pairs from the amine groups into the nitro groups leads to increasing polarity in the solid state. This enhances electrostatic N−O attractions between the NO_2 groups of adjacent molecules. For example, the shortest intermolecular N···O distances of ca. 3.0 and 3.3 Å found in crystalline TNSD and TNSU, respectively, give evidence for such interactions. Besides the intermolecular N···O nonbonded contacts, the theoretical and experimental geometries both have intramolecular O···H nonbonded contacts (i.e., hydrogen bonds) between the oxygen of NO_2 and the hydrogen of CH_2. There are 14 and 11 intramolecular hydrogen bonds less than 3.0 Å found in the crystalline TNSD and TNSU, and the closest distances are about 2.3 and 2.2 Å, respectively. The interactions are significant in view of suggestions that intramolecular hydrogen transfer is also a minor pathway for decomposition of these spiro nitramines and other nitramines.[13,14,48,49] However, there are large differences between the experimental and calculated C−H bonds. Besides the above solid-state effect, the fact that positions of the hydrogen atoms are difficult to determine via X-ray diffraction is another reason for the bonds involving H atoms having larger discrepancies than the other bonds.

Moreover, we also find that both the number of the substituents and the ring size have important influences on the geometries. With the number of nitramine groups increasing, the average value of the C−C bond length as for the molecules **1**−**5** decreases, while average values of the C−N and N−N/N−NO_2 bond lengths increase in general because of the increase of the ring strain and the intramolecular interactions as mentioned above. However, there exist exceptions for the C−N bonds of *o*-DNSP and TeNSP. This may be attributed to their higher molecular symmetries D_2 and S_4. As for the structures containing the same nitramine groups (i.e., species **5**−**12**), as the ring size increases, average values of the C−C, C−N, and N−N/N−NO_2 bond lengths all decrease in general. This is because the ring strain and intramolecular interactions all decrease when the ring size becomes larger. Furthermore, the relative positions of the nitramine groups also have important effects on the geometries. The C−C and N−NO_2 bonds of *o*-DNSP are longer than those of *m*-DNSP because of the larger steric hindrance and interactions between the nitro groups. All these reflect the substituent effect commendably. As a whole, variations of the C−C, C−N, and N−N/N−NO_2 bond lengths are much larger than other geometrical parameters with the changes of the ring size and the number and relative positions of the substituents. This indicates that these parameters are more sensitive to the environment than others.

3.2. Bond Orders. Bond overlap populations reflect the electron accumulations in the bonding region, and they can provide us detailed information about the chemical bonding. As a whole, the larger the population is, the greater the bonding overlap. Therefore, bonds with larger populations are relatively stronger and more resistant to rupture. It is known that Mulliken population analysis[50] suffers from some shortcomings, especially the basis set dependence. However, for the purpose of comparing trends in the electron distribution for homologous compounds at the same calculation condition, results derived from Mulliken population analysis are still meaningful. As our goal here is to draw the variation trend of electron distribution in very similar systems, the conclusion based on Mulliken population analysis would be reasonable. The bond orders of the spiro nitramines were obtained from the Mulliken population analysis at the B3LYP/6-31G** level and collected in Table 3.

Inspecting the data in Table 3, it can be found that the variations of bond overlap populations are consistent with those of the geometric parameters, and they are also affected by the number and relative positions of nitramine groups and the ring

TABLE 4: Thermodynamic Properties of the Title Compounds at Different Temperatures

	T (K)	200.0	273.15	298.15	400.0	600.0	800.0
NSP	$C^\circ_{p,m}$ (J·mol^{-1}·K^{-1})	86.32	112.03	121.08	155.73	205.95	237.95
	S°_m (J·mol^{-1}·K^{-1})	311.49	342.13	352.33	392.87	466.29	530.24
	H°_m(kJ·mol^{-1})	11.41	18.65	21.57	35.70	72.26	116.87
m-DNSP	$C^\circ_{p,m}$ (J·mol^{-1}·K^{-1})	112.84	142.82	152.90	190.27	242.52	274.40
	S°_m (J·mol^{-1}·K^{-1})	359.84	399.44	412.38	462.70	550.61	625.10
	H°_m(kJ·mol^{-1})	14.79	24.14	27.84	45.37	89.09	141.03
o-DNSP	$C^\circ_{p,m}$ (J·mol^{-1}·K^{-1})	116.97	146.85	156.86	193.71	244.73	275.80
	S°_m (J·mol^{-1}·K^{-1})	362.73	403.60	416.89	468.31	557.37	632.37
	H°_m(kJ·mol^{-1})	15.24	24.89	28.68	46.60	90.88	143.17
TriNSP	$C^\circ_{p,m}$ (J·mol^{-1}·K^{-1})	144.61	178.59	189.55	228.86	281.56	312.40
	S°_m (J·mol^{-1}·K^{-1})	414.48	464.62	480.74	542.15	645.88	731.47
	H°_m(kJ·mol^{-1})	19.01	30.84	35.44	56.83	108.35	168.01
TeNSP	$C^\circ_{p,m}$ (J·mol^{-1}·K^{-1})	177.78	215.57	227.35	268.24	320.92	350.51
	S°_m (J·mol^{-1}·K^{-1})	473.22	534.33	553.72	626.51	746.27	843.03
	H°_m(kJ·mol^{-1})	23.60	38.01	43.55	68.88	128.31	195.73
TNSHe	$C^\circ_{p,m}$ (J·mol^{-1}·K^{-1})	183.81	225.72	239.34	288.76	356.18	395.70
	S°_m (J·mol^{-1}·K^{-1})	468.79	532.33	552.69	630.18	761.21	869.58
	H°_m(kJ·mol^{-1})	23.70	38.69	44.50	71.49	136.58	212.11
TNSH	$C^\circ_{p,m}$ (J·mol^{-1}·K^{-1})	190.91	236.50	251.81	309.30	391.17	440.64
	S°_m (J·mol^{-1}·K^{-1})	476.57	542.81	564.19	646.45	788.69	908.58
	H°_m(kJ·mol^{-1})	24.30	39.94	46.04	74.70	145.42	229.00
TNSO	$C^\circ_{p,m}$ (J·mol^{-1}·K^{-1})	199.13	251.15	268.64	334.52	429.23	487.41
	S°_m (J·mol^{-1}·K^{-1})	469.78	539.54	562.29	650.69	805.76	937.87
	H°_m(kJ·mol^{-1})	24.29	40.76	47.26	78.06	155.20	247.32
TNSN	$C^\circ_{p,m}$ (J·mol^{-1}·K^{-1})	209.02	266.27	285.68	359.41	466.79	533.81
	S°_m (J·mol^{-1}·K^{-1})	492.73	566.32	590.48	685.00	852.70	996.90
	H°_m(kJ·mol^{-1})	25.54	42.92	49.82	82.76	166.21	266.78
TNSD	$C^\circ_{p,m}$ (J·mol^{-1}·K^{-1})	218.81	283.12	304.83	386.99	506.53	581.76
	S°_m (J·mol^{-1}·K^{-1})	498.26	575.95	601.69	703.05	884.41	1041.23
	H°_m(kJ·mol^{-1})	26.14	44.50	51.85	87.19	177.46	286.84
TNSU	$C^\circ_{p,m}$ (J·mol^{-1}·K^{-1})	235.67	302.42	325.30	413.28	544.37	628.46
	S°_m (J·mol^{-1}·K^{-1})	528.30	611.58	639.05	747.21	941.49	1110.47
	H°_m(kJ·mol^{-1})	28.58	48.25	56.10	93.81	190.53	308.41
TNSDo	$C^\circ_{p,m}$ (J·mol^{-1}·K^{-1})	247.65	320.08	344.89	440.43	583.45	675.88
	S°_m (J·mol^{-1}·K^{-1})	539.28	627.13	656.24	771.23	978.91	1160.35
	H°_m(kJ·mol^{-1})	29.58	50.33	58.65	98.74	202.15	328.74

size. With respect to the smaller five molecules **1**−**5**, with the number of nitramine groups increasing, average populations of the C−C, C−N, and N−N/N−NO_2 bonds decrease as expected, while those of the N−O and C−H bonds almost remain unchanged. This suggests that the stability of the title compounds decreases and their sensitivities increase accordingly. Obviously, this is caused by the strain energy on the skeleton and interactions among the nitro groups. Moreover, from mono- to tetrasubstituted spiro nitramines, populations of the C−N bonds are generally smaller than those of the N−NO_2 bonds, and the N−N bonds on the ring in some molecules are the weakest ones compared with other bonds, even with negative bonding populations. The negative values reflect that there obviously exist very strong ring strain and repulsion between the substituents, and the larger the absolute values of the negative bonding populations are, the stronger the repulsion. According to "the principle of the smallest bond order" (PSBO),[51] we infer that the N−N bonds on the ring are more fragile than other bonds in these molecules, and these bonds could be ruptured initially in their thermal decompositions. This is different from previous studies on the pyrolysis mechanisms of the usual nitramines.[3,13,14,48,49] Furthermore, it is also possible for these molecules to be pyrolyzed by initially breaking the C−N bond rather than the N−NO_2 bond in the decomposition process.

As for structures **5**−**12** containing the same nitramine groups, average populations of the C−C, C−N, and N−N/N−NO_2 bonds all increase, and those of the N−O and C−H bonds also remain almost unchanged with the increasing ring size. This indicates that the stability of the title compounds increase. Thus, the title compounds are relatively stable for thermolysis or stimulation, since the ring strain and intramolecular interactions decrease. Comparison of their bond overlap populations shows that the N−NO_2 bonds in molecules **7**−**12** are the weakest ones and may be initially broken in the pyrolysis and explosion, which agrees with the conclusion drawn from the previous studies. However, for the molecules TeNSP (**5**) and TNSHe (**6**), the N−N bonds on the ring skeleton are the least stable, followed by the C−N bond and then the N−NO_2 bond. So, breaking the N−N bonds on the ring skeleton may be the initial step in the thermolysis of the two molecules.

Additionally, it is found that the populations of the isomers are also affected by the relative positions of the substituents. As for *m*-DNSP and *o*-DNSP, populations of the C−C, C−N, and N−NO_2 bonds in the former are larger than those in the latter, which is consistent with the geometrical variations. This also implies the extent of the intramolecular interactions mainly caused by the nitramine groups.

3.3. Thermodynamic Properties. On the basis of vibrational analysis and statistical thermodynamic method, heat capacities ($C^\circ_{p,m}$), entropies (S°_m), and enthalpies (H°_m) ranging from 200 to 800 K were obtained and listed in Table 4. The scaled B3LYP/6-31G** harmonic vibrational frequencies (in cm^{-1}) and their corresponding intensities (in km/mol) of the title compounds were given in Table 1S of the Supporting Information. Since there are no corresponding experimental values, we cannot make any comparison. The calculated thermodynamic functions and the established dependences of them on the temperature and the number of nitramine groups would be helpful for further studies on other physical, chemical, and energetic properties of the spiro nitramines.

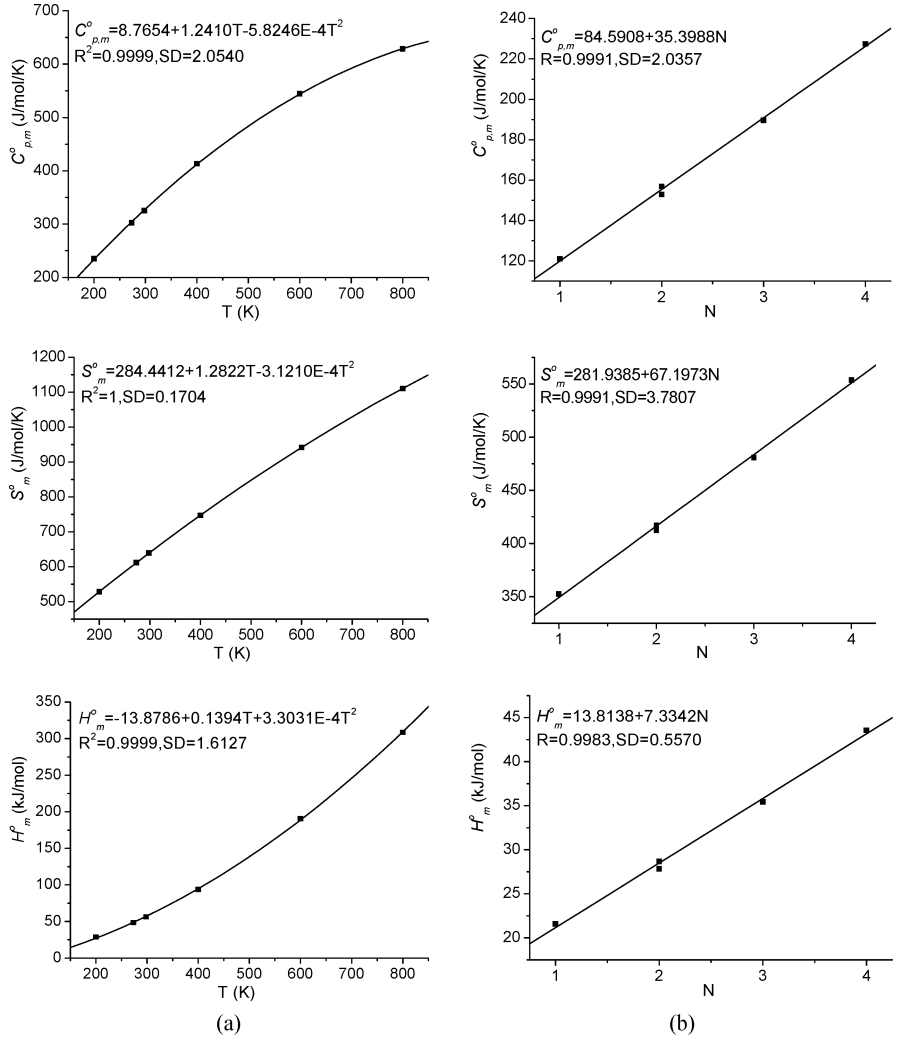

Figure 2. The relationships between the thermodynamic functions ($C^{\circ}_{p,m}$, S°_{m}, and H°_{m}) and the temperature (T) (a) and the number of the nitramine groups (N) (b).

As can be seen from Table 4, the thermodynamic properties of spiro nitramines all evidently increase as the temperature increases. This is because the vibrational movement is intensified at higher temperature and makes more contributions to the thermodynamic functions, while at lower temperature, the main contributions to the thermodynamic functions come from the translations and rotations of the molecules. Taking TNSU as an example, the relationships between the thermodynamic functions and the temperature in the range 200−800 K can be expressed as in Figure 2a. It is obvious that, when the temperature increases, the increments for both $C^{\circ}_{p,m}$ and S°_{m} decrease but increases constantly for H°_{m}.

In addition, all the thermodynamic functions increase with both the increasing ring size and number of nitramine groups. We deduce that, when the ring becomes larger or more nitramine groups are attached to the ring, these thermodynamic functions will probably keep on increasing. With molecules **1**−**5** as examples, the relationships between the thermodynamic properties and the number of the substituents at 298.15 K are shown in Figure 2b. One could find that, on average, $C^{\circ}_{p,m}$, S°_{m} and H°_{m} increase by 35.4 J·mol^{-1}·K^{-1}, 67.2 J·mol^{-1}·K^{-1}, and 7.3 kJ·mol^{-1}, respectively, when one more nitroamino group is attached. This shows good group additivity on the thermodynamic functions. The relative positions of the nitramine groups also have important effects on the thermodynamic properties. For example, for *m*-DNSP and *o*-DNSP, three thermodynamic functions of the former are smaller than those of the latter, which is because the nitramine groups of *o*-DNSP in closer distance leads to the stronger intramolecular interactions. This can be exhibited and elucidated by their vibrational modes (Table 1S), too. The frequencies at 1302 and 1312 cm^{-1} and 1673 and 1684 cm^{-1} are associated with the typical N−NO$_2$ symmetric and asymmetric stretching vibrations of *o*-DNSP, respectively, and they are also associated with very strong adsorption intensities. However, with respect to *m*-DNSP, there exist slight red-shifts for the corresponding frequencies. The N−NO$_2$ symmetric and asymmetric stretching vibrational modes have decreased to 1294 and 1308 cm^{-1} and 1637 and 1649 cm^{-1}, respectively. And, in comparison with the corresponding vibrational intensities in *o*-DNSP, those in *m*-DNSP are somewhat evenly distributed, i.e., the high intensity decreases while the low intensity increases. The characteristic C−H stretching modes of *o*-DNSP are also in higher frequency ranges (3028−3122 cm^{-1}) than those of *m*-DNSP (3017−3112 cm^{-1}).

3.4. Detonation Properties. Table 5 collects the predicted and available experimental ρ, D, and P of the title compounds, RDX and HMX. The oxygen balances (OB_{100}) and heats of formation (HOF) were also calculated and listed in this table. Here, it should be pointed out that HOF of the title compounds were obtained directly from the semiempirical PM3 MO method and used to estimate the detonation energy (Q). Previous studies[52] have reported and proven that HOF calculated by the

TABLE 5: Predicted Densities and Detonation Properties of the Title Compounds and Other Famous Nitramine Explosives[a]

no.	compd	OB_{100}	HOF[b] (kJ/mol)	Q (kJ/g)	V[c] (cm^3/mol)	ρ (g/cm^3)	D (km/s)	P (GPa)
1	NSP	−8.76	265.98	1570.17	78.95	1.45	6.92	18.47
2	*m*-DNSP	−1.25	367.27	1857.74	97.32	1.65	8.42	29.78
3	*o*-DNSP	−1.25	418.96	1934.90	96.39	1.66	8.53	30.74
4	TriNSP	2.91	530.53	1808.36	109.84	1.88	9.56	41.57
5	TeNSP	5.55	701.66	1038.31	128.12	1.97	8.62	34.71
6	TNSHe	3.76	500.23	1373.29	135.98	1.96	9.22	39.62
7	TNSH	2.14	306.12	1680.98	149.68	1.87	9.39	40.04
8	TNSO	0.68	264.80	1603.89	155.51	1.89	9.22	38.97
9	TNSN	−0.65	227.05	1536.58	167.82	1.84	8.82	34.97
10	TNSD	−1.86	231.27	1506.26	178.98	1.80 (1.71)	8.53	32.26
11	TNSU	−2.97	229.47	1474.20	191.11	1.76 (1.74)	8.24	29.68
12	TNSDo	−4.00	217.86	1438.01	207.46	1.69	7.86	26.34
13	RDX	0.00	168.90	1597.39	124.92	1.78 (1.81)	8.88 (8.75)	34.75 (34.70)
14	HMX	0.00	270.41	1633.88	157.53	1.88 (1.90)	9.28 (9.10)	39.21 (39.00)

[a] Data in the parentheses are the experimental values taken from refs 2, 11. [b] Heat of formation obtained from the calculation at the PM3 level. [c] Average volume from 100 single-point volume calculations at the B3LYP/6-31G** level.

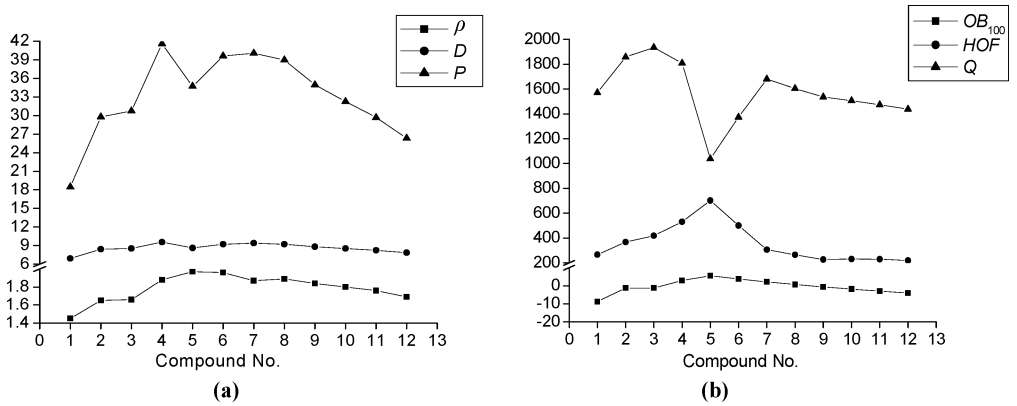

Figure 3. Correlations between the structures and the predicted explosive performances: (a) density (ρ), detonation velocity (D), and detonation pressure (P); (b) oxygen balance (OB_{100}), heat of formation (HOF), and detonation energy (Q).

PM3 method could replace the experimental data reasonably in evaluating the D and P of the energetic compounds, because they are not sensitive to the HOF but are quite sensitive to the ρ.

The calculated detonation properties agree well with the available experimental values.[2,11] For example, the relative errors for the estimated densities of TNSD, TNSU, RDX, and HMX are 5.26%, 1.15%, −1.66%, and −1.05%, respectively. The evaluated detonation velocities of RDX and HMX compare favorably with the experimental values within errors 1.49% and 1.98%, while their errors for the evaluated detonation pressures are only 0.14% and 0.54%, respectively. All these reflect that our predictions of the detonation properties for the title compounds are reliable and further confirm the reliability of the calculation method chosen for these molecular systems.

To show the relationships more clearly between the structures and the detonation properties, we reproduced the data from Table 5 in Figure 3. It was noticed that from monosubstituted spiropentane to tetrasubstituted, ρ, D, and P all increase with the increasing number of nitramine groups, as well as the OB_{100} and HOF, except for TeNSP. This obviously shows good group additivity on the detonation properties and also strongly supports the claim that introducing more nitro substituents (moderately increasing the oxygen balance) into an energetic molecule usually helps to increase its detonation performance. The exception for TeNSP is that it has the highest OB_{100}, HOF, and ρ but abnormally lower D and P. The most positive oxygen balance of TeNSP deviates largely from the perfect oxygen balance, which leads to the lowest Q and decreases the performances of D and P. The same is true for TNSHe. The relative positions of nitramine groups also have an important effect on the explosive properties of energetic materials. For example, *o*-DNSP has higher HOF, Q, ρ, D, and P than *m*-DNSP, since the former has a more compact structure and larger strain energy than the latter. As for molecules **5**−**12**, OB_{100}, HOF, ρ, D, and P all decrease with the increasing ring size in general. This is attributed to the increasing molecular volume and decreasing ring strain when the ring size increases. The exception of TNSHe has been discussed above. This is consistent with a previous study[53] in which correlation between the oxygen balance and the detonation performances will break down if the explosives have more positive OB_{100}, but there are better correlations between the OB_{100}, HOF, and ρ.

In comparison with the commonly used explosives RDX and HMX, TriNSP, TNSHe, TNSH, and TNSO can be considered potential candidates of HEDMs. They have the predicted densities of ca. 1.9 g/cm^3, detonation velocities over 9 km/s, and detonation pressures of about 39 GPa and even over 40 GPa. In addition, in comparison with another famous nitroaromatic explosive TNT (trinitrotoluene) (ρ = 1.64 g/cm^3, D = 6.95 km/s, P = 19.0 GPa),[2] the spiro nitramines studied in this paper except NSP all have better detonation performance than it. Therefore, if these stable spiro nitramines can be synthesized, they will have higher exploitable values and be worth investigating further.

3.5. Thermal Stability and Pyrolysis Mechanism. Another main concern for the energetic materials is whether they are kinetically stable enough to be of practical interest. Thus, studies on the bond dissociation or pyrolysis mechanism are important and essential for understanding the decomposition process of

TABLE 6: Comparison of Theoretical Bond Dissociation Energies (BDE, kcal/mol) for Typical C−C, C−N, and N−N Bonds at G2 and B3LYP/6-31G Levels**

compd	CH_3-CH_3	CH_3-NO_2	NH_2-NO_2	$(CH_3)_2N-NO_2$	CH_3NH-NO_2[b]
G2	88.30	61.00	51.08(51.1)[b]	49.15	51.7
B3LYP/6-31G**	86.31	54.52(54.6)[a]	47.03(47.0)[a]	41.13	44.5

[a] ref 23. [b] ref 24.

TABLE 7: Bond Dissociation Energies (BDE, kcal/mol) for the C−C, C−N, N−N, and N−NO_2 Bonds of the Title Compounds Computed at the (U)B3LYP/6-31G Level[a]**

		BDE^0				BDE			
no.	compd.	C−C	C−N	N−N	N−NO_2	C−C	C−N	N−N	N−NO_2
1	NSP	50.34	38.86		36.79	45.84[b]	35.27		32.11
2	*m*-DNSP	48.02	46.81		35.33	44.83	44.59		30.79
3	*o*-DNSP	47.33	44.22	21.40	27.43	42.66	42.33[b]	19.55	23.37
4	TriNSP	46.88	41.35	18.94	24.55	43.49	40.18[b]	17.15	20.46
5	TeNSP		38.04	22.65	27.66		36.76[b]	20.64	24.79[b]
6	TNSHe		30.07	23.95	26.46		29.06[b]	22.13	23.26[b]
7	TNSH		50.14		37.92		47.24		33.63
8	TNSO	66.05	50.11		38.78	61.37	46.76		34.12
9	TNSN	67.85	69.08		36.47	62.81	64.84		31.69
10	TNSD	62.39	61.78		27.10	57.38	57.92		22.22
11	TNSU	70.26	73.27		43.50	65.77	68.19		38.40
12	TNSDo	78.01	81.51		43.09	72.86	75.90		37.86
13	RDX		73.99		41.86		68.66		36.76 (36.35)[c]
14	HMX		70.93		44.43		65.59		39.79

[a] BDE^0 denotes the bond dissociation energies without zero-point energy corrections, while BDE denotes the bond dissociation energies including zero-point energy corrections. [b] These BDE were obtained from treating the N−NO_2 bond with a fixed length adjacent the dissociation bond; otherwise, these bond dissociations cannot be done. This is due to the strong ring strain and high molecular symmetries of the parent species, which leads to the instability of the corresponding radicals. [c] ref 24.

the energetic materials, since they are directly relevant to the sensitivity and stability of the energetic compounds. Previous studies[21−25] on the BDE for the nitro compounds such as nitroaromatic and nitramine molecules have shown that there is a parallel relationship between the BDE for the weakest R−NO_2 bond scission in the molecule and its sensitivity. Usually, the larger the BDE value for scission of the R−NO_2 bond is, the lower the sensitivity. Thus, the calculated BDE for removal of the NO_2 group can be used to index the relative sensitivity of the nitro molecules. However, this is only applied to the molecules in which the R−NO_2 bond is the weakest one. For example, the C−C bond of nitrocubanes is weaker than the C−NO_2 bonds, and the initial step in decomposition is rupture of the cube C−C bond.[54] Thus, in such molecules, the R−NO_2 scission should not be used as an index of sensitivity. Similarly, in the present research, the weakest bond in some spiro nitramine molecules may not be the N−NO_2 bond. So, four possible bond dissociations were considered here to elucidate the pyrolysis mechanisms and relative stabilities of the title compounds: (1) the C−C bond on the ring skeleton; (2) the C−N bond on the ring; (3) the N−N bond on the ring; and (4) the N−NO_2 bond on the side chain. It should be pointed out that we selected the weakest C−C, C−N, N−N, and N−NO_2 bonds as the breaking bond based on the Mulliken bonding population analyses at the B3LYP/6-31G** level.

First, a benchmark calculation on several small molecules with C−C, C−N, and N−N bonds by using Gaussian-2 (G2) theory[55] was carried out to check the accuracy of BDE computed with the B3LYP/6-31G** method. The G2 theory is an approximation to the QCISD(T)/6-311+G(3df,2p)// MP2/6-31G* level of theory, and intended to calculate atomization energies accurate to within 1−2 kcal/mol.[55] Table 6 summarizes the computed BDE values at the G2 and B3LYP/6-31G** levels. Figure 4 shows a very good linear relationship between the B3LYP/6-31G** and G2 calculated BDE values ($R = 0.9965$, SD = 1.5867). As can also be noticed in Table 6, the B3LYP/6-31G** theory slightly underestimates C−C, C−N, and N−N bond strengths compared with the high-level G2 theory, which is not surprising and is in line with the previous studies.[24,56] On this basis, we might expect reliable calculated results for the large spiro nitramines.

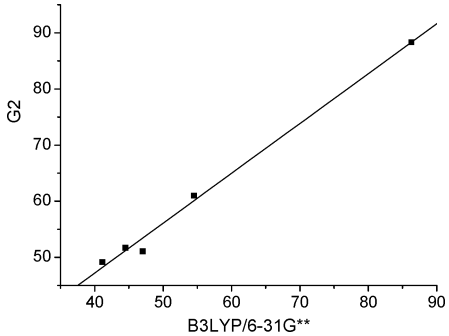

Figure 4. Comparison of the BDE calculated by the B3LYP/6-31G** theory and G2 theory.

The BDE of low-energy fragmentation pathways for the title compounds at the B3LYP/6-31G** level were listed in Table 7, while the calculated energetic data of the parent nitramines and the corresponding bond dissociation products were summarized in Table 2S of the Supporting Information for brevity. From Table 7, at first we can find that the fragmentation pathways are not affected by the zero-point vibrational energies. The dissociation energies are shifted toward lower energies by less than 6 kcal/mol when the zero-point vibrational energies are included. The calculated BDE of N−NO_2 bond scission for RDX (36.76 kcal/mol) agrees well the previous study (36.35 kcal/mol),[24] which further verifies the reliability of our calculated results for these structures with the B3LYP/6-31G** method. Second, on the basis of the calculated BDE, it was determined that the trigger linkage in all spiro nitramines appears to be N−N homolysis, but there are differences. As for the molecules with a N−N bond on the ring, the N−N bond is easier to break,

TABLE 8: Heats of Formation (HOF) for the Reactants (R) and Transition States (TS), and Activation Energies (E_a) for the Homolysis of C−C, C−N, N−N, and N−NO_2 Bonds in the Studied Species at the UHF−PM3 Level[a]

		HOF (kJ/mol)					E_a (kJ/mol)			
			TS							
no.	compd.	R	C−C	C−N	N−N	N−NO_2	C−C	C−N	N−N	N−NO_2
1	NSP	541.87	650.47	642.76		647.49	108.60	100.89		105.62
2	*m*-DNSP	614.50	747.02	727.24		722.22	132.52	112.74		107.72
3	*o*-DNSP	666.60	773.39	795.65	715.82	769.45	106.79	129.05	49.22	102.85
4	TriNSP	749.38	873.83	880.55	797.70	850.49	124.45	131.17	48.32	101.11
5	TeNSP	892.63		1019.48	941.07	1071.46		126.85	48.44	178.83
6	TNSHe	766.71		852.52	825.66	884.82		85.81	58.95	118.11
7	TNSH	648.14		794.78		759.17		146.64		111.03
8	TNSO	680.71	884.43	856.13		785.40	203.72	175.42		104.69
9	TNSN	715.22	895.64	912.30		794.68	180.42	197.08		79.46
10	TNSD	792.29	990.63	994.78		863.53	198.34	202.49		71.24
11	TNSU	865.43	1034.59	997.66		936.79	169.16	132.23		71.36
12	TNSDo	929.66	1097.77	1058.72		1003.04	168.11	129.06		73.38
13	RDX	520.90		757.68		599.12		236.78		78.22
14	HMX	739.34		910.36		806.36		171.02		67.02

[a] All the heats of formation have been corrected by the zero-point energy.

while the side N−NO_2 bond dissociation is easier for those spiro nitramines without a N−N bond on the ring skeleton. This suggests that homolysis of the N−N bond for the spiro nitramines with a N−N bond on the ring is the initial step in the thermolysis or explosion in the gas phase, while rupture of the side N−NO_2 bond is the initial step in the pyrolysis of other molecules without a N−N bond on ring. Obviously, this difference is caused by the strain energies on the skeleton, which agrees well with the above bond overlap population analysis and further gives the "PSBO" powerful support. On the other hand, the results also show that the C−C, C−N, and N−N bond strengths in the title compounds are all smaller than those in ethane, nitromethane, nitroamine, methylnitroamine, and dimethylnitroamine. Thus, initiation of the spiro nitramine decomposition by the N−N/N−NO_2 bond homolysis and propagation of the decomposition by other bond dissociations should be facile processes. The low N−N/N−NO_2 bond strength is a consequence of the electrostatic interactions and the σ electron-withdrawing NO_2 substituents in the cyclic nitramines.

In addition, on the basis of the BDE for the initial steps in their thermal decompositions, it can be deduced that the relative stability of these spiro nitramines may be in the order TNSU > TNSDo > TNSO > TNSH > NSP > TNSN > *m*-DNSP > TNSD > TNSHe > TeNSP > *o*-DNSP > TriNSP. On the whole, the stability decreases with the increasing nitramine groups, while it increases with the ring size increases, and the species with a N−N bond on the ring are more sensitive than others. However, there are some discrepancies which may be caused by various factors in the neutral molecules and the formed radicals. The relative positions of nitramine groups also have an important effect on the BDE. For example, *m*-DNSP has larger BDE than *o*-DNSP, since the distance between two nitramine groups in the former is shorter than that in the latter. So, *m*-DNSP is more stable than *o*-DNSP, which can also be judged from their total energies (Table 2S) and heats of formation (Table 5). Further, it is worth noting that the molecular symmetry has a significant influence on the BDE. As for TeNSP, TriNSP, and *o*-DNSP, their stability order (TeNSP > *o*-DNSP > TriNSP) agrees well with the order of their molecular symmetries $S_4 > D_2 > C_1$, i.e., the higher the symmetry, the more stable the molecule is. This disagrees with that derived from the group additivity as *o*-DNSP > TriNSP > TeNSP.

In comparison with the corresponding BDE of RDX and HMX, only TNSU and TNSDo have comparable thermal stability and sensitivity, while the others are less stable.

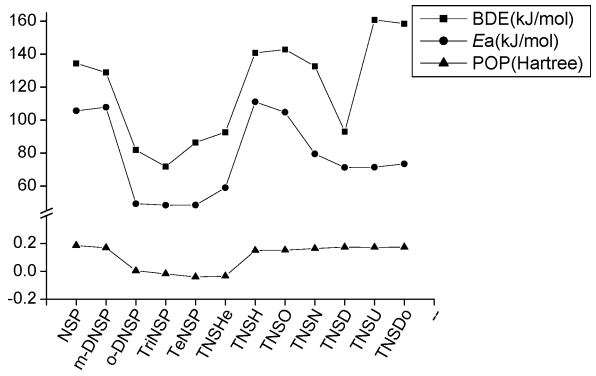

Figure 5. Relationship between the BDE, E_a, and bond overlap populations (POP) of the initial breaking bond in thermolysis processes of the spiro nitramines.

However, according to the suggestion of Chung et al.[57] that a molecule should have more than a 20 kcal/mol barrier to dissociate to be considered a viable candidate of HEDM, we can conclude that the molecules in Table 7 except *o*-DNSP and TriNSP are all viable candidates of HEDMs. In conjunction with the detonation performances (Table 5), it is evident that TNSHe, TNSH, and TNSO are the preferred candidates of HEDMs and thus have exploitable values.

Activation energies (E_a) of four possible initial steps in the pyrolysis reactions as above were investigated with the UHF−PM3 method and summarized in Table 8. Similarly, the lower the E_a for breaking a bond is, the greater the possibility of the bond breaking being the initial step, and the lower the stability of the corresponding compound. Comparison of the E_a for homolysis of various bonds gives the same conclusion as that drawn from the BDE at the B3LYP/6-31G** level. The N−NO_2 bond is the trigger bond in the pyrolysis reactions for the molecules with larger spiro rings and without N−N bond on the ring such as from TNSH to TNSDo, and the sensitivities of these molecules are relatively lower. While for other molecules such as *o*-DNSP, TriNSP, TeNSP, and TNSHe with a N−N bond on the ring skeleton, homolysis of the N−N bond may be the initial step, since the E_a for breaking this bond is much lower than those for breaking the other bonds. Therefore, according to the E_a of the initial steps, we can further infer that the species with N−N bonds on the ring are more sensitive than the others. However, probably because of the limitations of the calculation method, the calculated E_a by the UHF−PM3 method are all

lower than the corresponding BDE by the B3LYP method, and there are some discrepancies between the thermal stability order derived from the BDE, E_a, and bond overlap populations (see Figure 5). This shows that the UHF−PM3 method may only be used to study the pyrolysis mechanisms of the spiro nitramines qualitatively instead of quantitatively.

4. Conclusions

From the theoretical studies on a series of spiro nitramines, the following conclusions can be drawn:

1. The B3LYP/6-31G** method can generate reliable geometries of the spiro nitramines. The optimized structures of the title compounds agree reasonably with the experimental data, and the differences between the calculated and experimental values can be explained by the crystal packing effect. Most bond lengths generally increase little with the increasing number of nitramine groups but decrease when the ring size enlarges.

2. Variations of bond overlap populations are consistent with the geometric parameters, and they decrease with increasing substituents but increase with enlarging ring size. Intramolecular interactions appear to be the most straightforward factor leading to the smaller bonding populations of some molecules.

3. Thermodynamic properties all increase quantitatively with increasing temperature, number of nitramine groups, and ring size. The increments for heat capacities and entropies decrease, while they increase constantly for enthalpies as the temperature increases.

4. The predicted detonation properties are comparable to the experimental data. Density, detonation velocity, and detonation pressure of the spiro nitramines all increase with increasing number of nitramine groups, as well as the oxygen balance and heat of formation, in general, but decrease with enlarging ring size, except those with more positive oxygen balance. All molecules except NSP perform better than TNT. TNSO, TNSH, TNSHe, and TriNSP with superior detonation performances can be expected to be novel potential candidates of HEDMs compared with RDX and HMX.

5. Pyrolysis mechanisms of the spiro nitramines derived from the bond overlap populations, the bond dissociation energies at the B3LYP/6-31G** level, and the activation energies at the UHF−PM3 level are basically consistent. The initial step in the pyrolysis for the molecules with a N−N bond on the ring is homolysis of this bond; while for the other molecules without a N−N bond on the ring, the initial step is the side N−NO_2 bond homolysis. Stabilities of the title compounds decrease with increasing nitramine groups and increase with enlarging ring size, in general.

6. In comparison with the B3LYP/6-31G** BDE, the PM3 method underestimates the activation energies for the initial steps, and there are some discrepancies between the thermal stability order derived from the BDE and E_a. This shows that the UHF−PM3 method may only be used to study the pyrolysis mechanisms of the spiro nitramines qualitatively.

7. Considering thermal stability, only TNSO, TNSH, and TNSHe can be used as HEDMs with less sensitivity and higher performance and are worthy of further investigation. The dependence of the properties on structural changes of the spiro nitramines that were established in this work may be used to screen novel HEDMs efficiently.

Acknowledgment. We gratefully thank the National Natural Science Foundation of China (grants no. 10576030 and no. 10576016) for their support of this work.

Supporting Information Available: Optimized structures of spiro nitramines, gradient-corrected harmonic vibrational frequencies, and calculated total energies and zero-point energies. This material is available free of charge via the Internet at http://pubs.acs.org.

References and Notes

(1) Borman, S. *Chem. Eng. News* **1994**, *72*, 18.
(2) Olah, G. A.; Squire, D. R. *Chemistry of energetic materials*; Academic Press: San Diego, 1991.
(3) Xiao, H. M. *Molecular orbital theory for nitro compounds*; National Defence Industry Press: Beijing, 1993.
(4) Kamlet, M. J.; Jacobs, S. J. *J. Chem. Phys.* **1968**, *48*, 23.
(5) Willer, R. L. *Propellants, Explos., Pyrotech.* **1983**, *8*, 65.
(6) Nielsen, A. T.; Chafin, A. P.; Christian, S. L.; Moore, D. W.; Nadler, M. P.; Nissian, R. A.; Vanderah, D. J.; Gilardi, R. D.; George, C. F.; Flippen-Anderson, J. L. *Tetrahedron* **1998**, *54*, 11793.
(7) Willer, R. L. NWC-TM-4703, Naval Weapons Center, China Lake, CA, January, 1982.
(8) Willer, Rodney L. *Synthesis and characterization of new insensitive high energy polynitramine compound, 2,4,8,10-tetranitro-2,4,8,10-tetraazaspiro[5.5]undecane (TNSU)*. Report, NWC-TP-6353; Order No. AD-A116832, 16 pp. Avail. NTIS From: *Gov. Rep. Announce. Index (U. S.)* **1982**, *82*(23), 4839.
(9) Willer, R. L. U.S. Patent 4,485,237, 1984.
(10) Willer, R. L. *J. Org. Chem.* **1984**, *49*, 5147.
(11) Lowe-Ma, C. K. *Acta Crystallogr., Sect. C* **1990**, *46*, 1029.
(12) Lowe-Ma, C. K.; Willer, R. L. Private communication, 1990.
(13) Brill, T. B.; Oyumi, Y. *J. Phys. Chem.* **1986**, *90*, 6848.
(14) Oyumi, Y.; Brill, T. B. *Combust. Flame* **1987**, *68*, 209.
(15) Qiu, L.; Xiao, H. M.; Ju, X. H.; Gong, X. D. *Int. J. Quantum Chem.* **2005**, *105*, 48.
(16) Xiao, J. J.; Zhang, J.; Yang, D.; Xiao, H. M. *Acta Chim. Sin.* **2002**, *60*, 2110.
(17) Qiu, L.; Xiao, H. M.; Ju, X. H.; Gong, X. D. *Chin. J. Chem. Phys.* **2005**, *18*, 541.
(18) Qiu, L.; Xiao, H. M.; Ju, X. H.; Gong, X. D. *Acta Chim. Sin.* **2005**, *63*, 377.
(19) Xu, X. J.; Xiao, H. M.; Gong, X. D.; Ju, X. H.; Chen, Z. X. *J. Phys. Chem. A* **2005**, *109*, 11268.
(20) Parr, R. G.; Yang, W. *Density-functional Theory of Atoms and Molecules*; Oxford University Press: Oxford, 1989.
(21) Owens, F. J. *THEOCHEM* **1996**, *370*, 11.
(22) Politzer, P.; Murray, J. S. *THEOCHEM* **1996**, *376*, 419.
(23) Politzer, P.; Lane, P. *THEOCHEM* **1996**, *388*, 51.
(24) Harris, N. J.; Lammertsma, K. *J. Am. Chem. Soc.* **1997**, *119*, 6583.
(25) Rice, B. M.; Sahu, S.; Owens, F. J. *THEOCHEM* **2002**, *583*, 69.
(26) Saraf, S. R.; Rogers, W. J.; Mannan, M. S. *Ind. Eng. Chem. Res.* **2003**, *42*, 1341.
(27) Lu, W. C.; Wang, C. Z.; Nguyen, V.; Schmidt, M. W.; Gordon, M. S.; Ho, K. M. *J. Phys. Chem. A* **2003**, *107*, 6936.
(28) Colvin, K. D.; Strout, D. L. *J. Phys. Chem. A* **2005**, *109*, 8011.
(29) Becke, A. D. *J. Chem. Phys.* **1993**, *98*, 5648.
(30) Lee, C.; Yang, W.; Parr, R. G. *Phys. Rev. B* **1988**, *37*, 785.
(31) Hariharan, P. C.; Pople, J. A. *Theor. Chim. Acta* **1973**, *28*, 213.
(32) Frisch, M. J.; Trucks, G. W.; Schlegel, H. B.; Scuseria, G. E.; Robb, M. A.; Cheeseman, J. R.; Zakrzewski, V. G.; Montgomery, J. A.; Stratmann, R. E.; Burant, J. C.; Dapprich, S.; Millam, J. M.; Daniels, A. D.; Kudin, K. N.; Strain, M. C.; Farkas, O.; Tomasi, J.; Barone, V.; Cossi, M.; Cammi, R.; Mennucci, B.; Pomelli, C.; Adamo, C.; Clifford, S.; Ochterski, J.; Petersson, G. A.; Ayala, P. Y.; Cui, Q.; Morokuma, K.; Malick, D. K.; Rabuck, A. D.; Raghavachari, K.; Foresman, J. B.; Cioslowski, J.; Ortiz, J. V.; Stefanov, B. B.; Liu, G.; Liashenko, A.; Piskorz, P.; Komaromi, I.; Gomperts, R.; Martin, R. L.; Fox, D. J.; Keith, T.; Al-Laham, M. A.; Peng, C. Y.; Nanayakkara, A.; Gonzalez, C.; Challacombe, M.; Gill, P. M. W.; Johnson, B. G.; Chen, W.; Wong, M. W.; Andres, J. L.; Head-Gordon, M.; Replogle, E. S.; Pople, J. A. *Gaussian 98*, Revision A.11; Gaussian Inc.: Pittsburgh, PA, 2001.
(33) Scott, A. P.; Radom, L. *J. Phys. Chem.* **1996**, *100*, 16502.
(34) Hill, T. L. *Introduction to Statistical Thermodynamics*; Addision-Wesley Publishing Company: New York, 1960.
(35) Zhang, X. H.; Yun, Z. H. *Explosive chemistry*; National Defence Industry Press: Beijing, 1989.
(36) Qiu, L.; Xiao, H. M.; Xu, X. J.; Gong, X. D.; Ju, X. H. *J. Chem. Phys.*In review.
(37) Zhang, J.; Xiao, H. M. *J. Chem. Phys.* **2002**, *116*, 10674.
(38) Ju, X. H.; Xiao, J. J.; Li, Y.; Xiao, H. M. *Chin. J. Struct. Chem.* **2003**, *22*, 223.
(39) Liu, M. H.; Chen, C.; Hong, Y. S. *THEOCHEM* **2004**, *710*, 207.
(40) Lide, D. R., Ed. *CRC Handbook of Chemistry and Physics*; CRC Press LLC: Boca Raton, Florida, 2002.
(41) Stewart, J. J. P. *J. Comput. Chem.***1989**, *10*, 209.

(42) Dewar, M. J. S.; Zoebisch, E. G.; Healy, E. F.; Stewart, J. J. P. *J. Am. Chem. Soc.* **1985**, *107*, 3902.
(43) Dewar, M. J. S.; Thiel, W. J. *J. Am. Chem. Soc.* **1977**, *99*, 4899.
(44) Bingham, R. C.; Dewar, M. J. S.; Lo, D. H. *J. Am. Chem. Soc.* **1975**, *97*, 1285.
(45) (a) Fan, J. F.; Gu, Z. M.; Xiao, H. M. *THEOCHEM* **1996**, *365*, 246. (b) Xiao, H. M.; Fan, J. F.; Gong, X. D. *Propellants, Explos., Pyrotech.* **1997**, *22*, 360. (c) Fan, J. F.; Gu, Z. M.; Xiao, H. M.; Dong, H. S. *J. Phys. Org. Chem.* **1998**, *11*, 360. (d) Xiao, H. M.; Fan, J. F.; Gu, Z. M.; Dong, H. S. *Chem. Phys.* **1998**, *226*, 15.
(46) Stewart, J. J. P. *J. Comput.-Aided Mol. Des.* **1990**, *4*, 1.
(47) Karpowicz, R. J.; Brill, T. B. *J. Phys. Chem.* **1983**, *87*, 2109.
(48) Harris, N. J.; Lammertsma, K. *J. Phys. Chem. A* **1997**, *101*, 1370.
(49) (a) Oxley, J. C.; Kooh, A. B.; Szekeres, R.; Zheng, W. *J. Phys. Chem.* **1994**, *98*, 7004. (b) Oxley, J. C.; Hiskey, M.; Naud, D.; Szekeres, R. *J. Phys. Chem.* **1992**, *96*, 2505. (c) Capellos, C.; Papagiannakopoulos, P.; Liang, Y. L. *Chem. Phys. Lett.* **1989**, *164*, 533. (d) Zuckermann, H.; Greenblatt, G. D.; Haas, Y. *J. Phys. Chem.* **1987**, *91*, 5159.
(50) Mulliken, R. S. *J. Chem. Phys.* **1955**, *23*, 1833.
(51) Xiao, H. M.; Wang, Z. Y.; Yao, J. M. *Acta Chim. Sin.* **1985**, *43*, 14.
(52) (a) Goh, E. M.; Cho, S. G.; Park, B. S. *J. Def. Technol. Res.* **2000**, *6*, 91. (b) Dorsett, H.; White, A. Aeronautical and Maritime Research Laboratory, Defence Science & Technology Organization (DSTO). DSTO, Technical Report DSTO-GD-0253, Australia, 2000. (c) Sikder, A. K.; Maddala, G.; Agrawal, J. P.; Singh, H. *J. Hazard. Mater. A* **2001**, *84*, 1.
(53) Roth, J. *Encyclopedia of explosives and related items*; Large Caliber Weapon System Laboratory, Armament Research and Development Command, U.S. Army, Dover, NJ, 1978; Vol. 8, p 57.
(54) Owens, F. J. *THEOCHEM* **1999**, *460*, 137.
(55) Curtiss, L. A.; Carpenter, J. E.; Raghavachari, K.; Pople, J. A. *J. Chem. Phys.* **1991**, *94*, 7221.
(56) Harris, N. J.; Lammertsma, K. *J. Am. Chem. Soc.* **1996**, *118*, 8048.
(57) Chung, G. S.; Schmidt, M. W.; Gordon, M. S. *J. Phys. Chem. A* **2000**, *104*, 5647.